

Title:

**Low-frequency acoustic propagation loss in the Arctic Ocean: results of the Arctic Climate Observations using Underwater Sound experiment.**

Authors:

Alexander N. Gavrilov,

Centre for Marine Science and Technology, Curtin University of Technology, GPO Box U1987,  
Perth WA 6845, Australia

Peter N. Mikhalevsky<sup>a</sup>,

Science Applications International Corporation, 1710 SAIC Dr., McLean, Virginia, 22102

Uploaded to the JASA manuscript submission system: 03/05/2004

Running title: Propagation loss from the ACOUS experiment

**DISTRIBUTION STATEMENT A**  
Approved for Public Release  
Distribution Unlimited

---

<sup>a</sup> Electronic-mail: [peter@osg.saic.com](mailto:peter@osg.saic.com)

## **ABSTRACT**

Acoustic data from the Arctic Climate Observations using Underwater Sound (ACOUS) experiment are analyzed to determine the correlation between acoustic propagation loss and the seasonal variability of sea ice thickness. The objective of this research is to provide long-term synoptic monitoring of sea ice thickness, an important global climate variable, using acoustic remote sensing. As part of the ACOUS program an autonomous acoustic source deployed northwest of Franz Josef Land transmitted tomographic signals at 20.5 Hz once every four days from October 1998 until December 1999. These signals were received on a vertical array in the Lincoln Sea 1250 km away. Two of the signals transmitted in April 1999 were received on a vertical array at ice camp APLIS in the Chukchi Sea north of Point Barrow, Alaska, at a distance of approximately 2720 km from the source. Temporal variations of the modal propagation loss are examined. The influence of ice parameters, variations of the sound speed profile, and mode-coupling effects on the propagation losses of individual modes is studied. The experimental results are compared to the results of the earlier experiments and the theoretical prediction using numerical modeling.

PASC numbers: 43.30.Pc, 43.30. Hw, 43.30.Qd

## I. INTRODUCTION

Acoustic ice reflection and scattering have been subjects of many experimental and theoretical studies since the earlier 1960s, because the interaction of sound waves with the rough sea ice cover is the main factor that affects attenuation of acoustic signals propagated in the Arctic Ocean. The signal transmission loss increases rapidly with frequency due to ice scattering. Therefore long-range acoustic transmissions in the Arctic Ocean are possible only at low frequencies of tens of Hz, and consequently low-frequency acoustic propagation is of particular research interest. The total energy loss of transmitted signals was studied in several acoustic propagation experiments in the Arctic<sup>1-3</sup>. Attenuation of individual normal modes at low frequencies is much less investigated experimentally. Knowing the modal propagation loss is important, because this makes it possible to predict the range and depth dependence of the sound field. Moreover, theoretical models of acoustic ice reflection and scattering at low frequencies can be examined in more detail by comparing the results of numerical prediction for modal attenuation due to ice scattering with the modal propagation loss measured experimentally.

Propagation losses of individual modes in the signals transmitted over the entire Arctic Basin were measured for the first time in the Transarctic Acoustic Propagation (TAP) experiment<sup>4,5</sup> in 1994. The TAP experiment results provided us with important data that were used for verifying the most recent models of ice scattering, propagation loss, and reverberation<sup>6</sup>. However, the TAP measurements were conducted for a relatively short time period of a week in April, which did not allow us to study temporal variations of the modal propagation loss and modal attenuation with changes in the ice cover characteristics and, particularly, seasonal variations of the mean ice thickness and roughness along the path. If this correlation is

experimentally examined and determined, it would prove the capability of acoustics to remotely monitor the sea ice thickness year round over large regions of the Arctic Ocean.

Long-term acoustic transmissions on a stationary trans-Arctic path were conducted for the first time in the Arctic Climate Observations using Underwater Sound (ACOUS) experiment in 1998-1999. Acoustic observations on the path of 1250 km long from the Franz Victoria Strait to the Lincoln Sea lasted for 14 months. Two of the ACOUS signals were also received on a vertical array at ice camp APLIS drifting in the northern part of the Chukchi Sea 2750 km away from the source. Signal reception on vertical arrays allowed us to separate individual modes of the signals and analyze different parameters of the modes, including the modal propagation losses. The main goal of the ACOUS experiment was to study long-term changes in the ocean temperature and heat content along the trans-Arctic path by means of acoustic thermometry. In addition, the obtained data gave us an opportunity to investigate temporal variations of modal attenuation due to various factors including seasonal change in the sea ice characteristics, variations of the sound speed, and the mode coupling effects.

It is widely believed that scattering of acoustic energy from the rough ice cover is the only significant phenomenon that influences acoustic transmission losses and modal attenuation in particular in the deep Arctic Basin. When modeling acoustic transmission losses due to ice scattering, researchers commonly use certain sound speed profiles typical for the Arctic Basin. Although the Arctic sound speed profiles are generally upward refracting and look nearly alike in every region of the deep Arctic Basin, actually the important characteristics of the sound speed profile, such as the thickness and sharpness of the upper under-ice acoustic duct above the thermocline, vary considerably from one region to another one. Relatively small spatial and temporal variations of the sound speed profile may lead to significant change of the modal group

velocities and attenuation. The other factor that may affect strongly the modal propagation loss and, in certain cases, the total acoustic transmission loss is mode coupling over range-dependent sections of the acoustic path. The influence of these factors on the modal propagation loss on the ACOUS path is considered in this paper along with the analysis of the temporal variations of modal attenuation due to seasonal change in the ice characteristics. The results of numerical modeling are used to interpret the experimental observations.

## **II. ACOUS EXPERIMENT**

### **A. Experimental scheme**

The ACOUS experiment started in October 1998 with the installation of an autonomous acoustic source deployed at the northern edge of the Franz Victoria Strait approximately 200 km northwest of Franz Josef Land and an autonomous vertical receiving array deployed in the Lincoln Sea 1250 km away (Fig.1). Both the source and the receiving array were installed at the edge of the continental shelf. The source was moored at a depth of 60 m below the sea surface in water depth of 440 m and transmitted tomographic signals at the carrier frequency of 20.5 Hz with a  $\pm 60^\circ$  phase modulation by 10 periods of a 255-bit maximum length pseudo-random sequence (M-sequence). Every bit of the sequence consisted of 10 periods of the carrier frequency. The transmissions were scheduled to start at 00:00 GMT every four days. The total duration of the signals was about 20.7 minutes and the signal level was nominally 195 dB re. 1  $\mu$ Pa (effective) at 1 m. Two accelerometers installed on the membranes of the source measured the amplitude of oscillations at the very beginning of each transmission and then the emitting system controller adjusted the oscillation amplitude to the nominal level of the transmitted signal. The octal code of the modulating M-sequence is 703, if the adjusted amplitude corresponds to the nominal level

within 195-195.5 dB. Otherwise the signal should be modulated with a different M-sequence, of which the octal code is set according to the level-to-code reference table.

The acoustic signals from the source were received on the vertical array. This flexible array consisted of 8 hydrophones spaced at 70-m intervals starting at 12 m from the bottom and nearly filling the water column of 545 m deep. The array was also equipped with 5 self-recording micro-CTD's that recorded pressure, temperature, and salinity at five different depths every 10 minutes. In March 2001 the Lincoln Sea receiving array was recovered. Examination of the signal recordings on the array showed that the source operated suitably for 14 months from October 11, 1998 until December 8, 1999. For this time period the source transmitted a total of 107 signals. The M-sequence code was 703 in all of the transmitted signals, which meant that the level of the transmitted signal remained nearly nominal (195 dB) for all the period of acoustic observations.

On April 9 and 13, 1999, two recordings of the ACOUS transmissions were made on a vertical array at ice camp APLIS established at the northern edge of the Chukchi Sea to support the SCICEX-1999 expedition. This flexible array was suspended from sea ice and consisted of 8 equidistant hydrophones that spanned the water column from 150 to 675 m. The array tilt was tracked via an ice-mounted acoustic navigation system.

## **B. Environmental conditions**

The bathymetry and the typical sound speed profile along the acoustic path to the Lincoln Sea are shown in Fig.2. The path crosses the Eurasia continental slope, the Gakkel Ridge, the western edge of the Lomonosov Ridge and the Canadian continental slope. Both continental slopes are steep so that coupling of the acoustic modes propagated over the slopes is significant. The

Gakkel Ridge is not high enough to influence the low-order modes of a 20-Hz signal propagated in the Arctic upward refracting acoustic channel. The western edge of the Lomonosov Ridge rises up to a depth of 1300 m and influences some of the acoustic modes that carry a considerable portion of the energy of the propagated signals.

According to the recent concept of the Atlantic Intermediate Water (AIW) circulation in the Arctic Ocean <sup>7</sup> shown in Fig.1, the acoustic path crosses the major circulation gyre along the continental margins in the regions of the incoming flow north of the Barents Sea and the return flow north of the Canadian shelf. The path also crosses the secondary branches of AIW circulation along the Lomonosov and Gakkel Ridges. The AIW circulation along the major cyclonic gyre and the subsidiary gyres is assumed to occur with so-called boundary currents along the continental shelf and the sea ridges <sup>8</sup>. The core of the AIW flow along the Eurasia continental slope is clearly seen in the temperature section built along the acoustic path with the use of the available oceanographic data. A statistical analysis of the historical oceanographic data collected in the regions along the acoustic path has shown that the AIW temperature is most variable along the initial section of the acoustic path in the Nansen Basin, and, particularly, over the Eurasia continental slope. It was found that Atlantic waters in this region in the 1990s were noticeably warmer than that in 1970-80s. In the Fram Basin and the Lincoln Sea the temperature profiles are more stable and vary a small amount relative to the climatology profiles <sup>9</sup>.

The DMSP SSM/I data on ice concentration <sup>10</sup> show that during the experimental observations the sea surface was covered year-round with ice in every region along the acoustic path. The mean ice draft was expected to be approximately 2 m in the Nansen Basins in the so-called Arctic summer season (July-November) <sup>11,12</sup>. The other regions along the path and the

Arctic winter season (February - May) are not well represented with the recent submarine up-looking sonar data.

The acoustic path to APLIS crosses the Eurasia continental slope, the Lomonosov and Mendelejev Ridges, and the Chukchi Plateau (Fig.3). The Lomonosov and Mendelejev Ridges do not rise above a depth of 1000 m and therefore do not influence the lower modes of the ACOUS signal. The sea floor topography in the region of the Chukchi Plateau is very uneven. The acoustic path crossed some parts of the plateau over which the depth was less than 600 m and hence the sea floor influenced considerably every mode of the ACOUS signal except for mode 1. The Scientific Ice Expeditions (SCICEX) oceanographic transect conducted by USS Hawkbill in April 1999 was almost coincident with the ACOUS path to APLIS and made right after the ACOUS signal receptions at APLIS. Therefore the sound speed profiles were well defined everywhere along the acoustic path except for the initial 400-km section that was not spanned by the oceanographic section. The oceanographic data collected in the regions along this section in the 1990s and the SCICEX-1999 data were used to synthesize the sound speed section along the acoustic path (shown in Fig.3) for numerical modeling of the ACOUS signal propagation. In April 1999, every region along the ACOUS path to APLIS was almost entirely covered with sea ice. Since the upward looking sonar data on ice draft collected in the SCICEX-1999 expedition were unavailable for us, we used the data of the earlier submarine cruises<sup>13</sup> to estimate the ice statistics parameters for modeling acoustic propagation along the path.

### **III. MODEL OF THE ACOUS SIGNAL PROPAGATION**

#### **A. Ice scattering loss**

The coherent reflection coefficient from Arctic sea ice was computed with the use of Kudryshov's ice scattering model<sup>14</sup>, of which a practical implementation is discussed in Ref.15.

Proper determination of the ice statistic characteristics including the roughness spectrum is critical for ice reflection modeling<sup>16</sup>. The morphological characteristics of the Arctic ice canopy have changed substantially over the last 2 decades<sup>11</sup>. Therefore we analyzed the data on Arctic ice draft which were available from the most recent submarine upward-looking sonar observations, in order to determine the most likely spectrum of the ice roughness and the typical numbers of mean ice thickness, standard deviation, and roughness correlation length. The analysis showed that the spectral fall-off rate of 2 is most probable for a 1-D ice draft profile in the Arctic winter season, while it is somewhat smaller and less definite in the summer season (Fig.4). For the Goff-Jordan model of the roughness spectrum<sup>17</sup>, the frequency dependence  $f^2$  of a 1-D roughness spectrum corresponds to a fractal dimension of 2.5 and the normalized 2-D power spectrum

$$G(\mathbf{u}) = (2\pi)^{-2} l_0^2 [1 + (\mathbf{u} l_0)^2]^{-3/2}, \quad (1)$$

where  $l_0$  is the roughness correlation length. The roughness power spectrum (1) corresponds to azimuthal isotropic roughness with the correlation function  $R(l) = \exp(-|r|/l_0)$ . Figure 5 shows an example of the measured power spectrum of ice draft roughness and its approximation by the model power spectrum that corresponds to the exponential correlation function.

The distribution of the ice roughness correlation length, derived from the ice draft data, is demonstrated in Fig.6. In the winter season, the ice roughness correlation length of 35-40 m is apparently most likely. In Arctic summer, the correlation length of about 40 m is also frequent, but the variance is much greater than that in winter. A large variance of the ice roughness correlation length is the consequence of ice-free zones spreading in summer.

The ice statistic parameters, such as mean ice draft (mean thickness) and roughness standard deviation, vary considerably over the Arctic Ocean regions and the seasons. According to the most recent observations, in winter the mean ice thickness is about 2-3 m in the Canada Basin and the Beaufort Sea and 3 - 4 m in the Fram and Nansen Basins. In summer, the mean ice thickness decreases to 1.5-2 m in the Canada Basin and 2-3 m in the Fram and Nansen Basins. In contrast to the ice thickness, the relationship between the roughness standard deviation and the mean thickness of ice is much less variable. In winter, the standard deviation is most likely 0.6 - 0.65 of the mean thickness, which is shown in Fig.7(a). In summer the values from 0.5 to 0.7 are almost equiprobable (Fig.7(b)).

Roughness of the top surface of the Arctic ice cover is also taken into account in Kudryashov's ice scattering model. Mutual statistical characteristics of the top and bottom ice roughness are poorly investigated. It is assumed in some recent ice scattering models<sup>16,18</sup> that the top and bottom scattering surfaces of Arctic ice are uncorrelated with each other. However, according to the Archimedean principle, the roughness of both surfaces of a floating ice sheet must be partly correlated and have similar spectra especially at smaller wavenumbers that correspond to the spatial periods larger than the ice thickness. Local observations at drifting ice stations North Pole have shown that the correlation between the top and bottom ice roughness is about 0.7, and the standard deviation of the top surface is about four times less than that of the bottom surface. Although these observations were quite local and sparse, and hence, could not create a representative statistical assembly, we used these estimates in the ice scattering model in the absence of more reliable data.

Figure 8(a) demonstrates the magnitude of the ice reflection coefficient versus grazing angle calculated at six frequencies, spaced at 4 Hz from 16 Hz to 36 Hz, for the ice parameters

expected in winter in the Central Arctic Basin. Small spikes at a grazing angle of  $60^{\circ}$  coincide with the critical angle for the longitudinal waves in ice. The angular dependence of the coherent ice reflection coefficient shown in Fig.8(b) was calculated for the typical ice characteristics observed in the Nansen Basin in August-October in the 1990s. The modal attenuation coefficients along the ACOUS paths were calculated for the typical sound speed profiles using KRAKENC code<sup>19</sup> with the modeled ice reflection coefficients as the top boundary conditions. Figures 9(a) and 9(b) show the variation of the attenuation coefficients of modes 1-5 at 20.5 Hz along the path to the Lincoln Sea calculated for the ice parameters given in the captions of Figs 8(a) and 8(b) respectively. The total propagation loss of modes on the path are given in these figures. It is evident from the comparison of modeling results in Fig.9, that seasonal change of the ice cover may lead to noticeable change in the modal propagation loss on a 1-Mm transarctic path, especially for mode 1. Note that the attenuation coefficient of individual modes also varies with the horizontal variation of the sound speed profile along the path, which results in variation of the modal cycle length. Substantial change of the modal attenuation due to sound speed variations will be discussed in more details in the next section.

It is evident that the ice statistic parameters, such as mean thickness and standard deviation, were not uniform along the ACOUS path to the Lincoln Sea. It is known from the earlier observations of ice draft in the 1970-1980s that the mean thickness and standard deviation of sea ice in the Lincoln Sea and the adjacent regions were larger than those in the Nansen and Fram Basins. However, wide-ranging observations of ice draft north of Greenland and the Canadian Archipelago were not conducted in the 1990s. Therefore, when modeling the ACOUS signal propagation, we assumed that the ice cover along the final 300-400 km section of the acoustic path might be somewhat thicker than that in the Nansen Basin.

## **B. Effects of mode coupling and variation of the sound speed profile**

The propagation of an acoustic signal at 20 Hz from the Franz Victoria Strait to the Lincoln was modeled earlier, before the experiment, using the climatology sound speed profiles and the ETOPO5 bathymetry database. The coupled-mode algorithm used for numerical modeling and the results of modeling are thoroughly considered in Ref.20, where it is shown that the mode coupling influences considerably the modal propagation loss along the path. It is also shown in Ref.20 that temporal variations of the sound speed over any, rapidly or slowly varying section of the path may lead to large variations of the modal propagation loss due to changes in the mode coupling effects. The newer modeling results presented below were obtained for the actual location of the ACOUS source and the Lincoln Sea array with the use of the recent International Bathymetry Chart of the Arctic Ocean (IBCAO) database<sup>21</sup> that is much more accurate than ETOPO5. Moreover the real sound speed profiles used in the new model are much more realistic than the climatology data.

Acoustic interaction with the sea floor plays a significant role in attenuation of the signals propagated over shallow-water sections of the acoustic path. For the ACOUS paths, such sections are the northern edge of the Franz Victoria Strait with the Eurasia continental slope, the northern edge of the Lincoln Sea with the Canada continental slope, and the Chukchi Plateau. Over these regions almost every mode of the ACOUS signal underwent significant interaction with the seabed. In the deep basins, interaction of the ACOUS signals with the seabed was negligible. Acoustic properties of the seabed in the Lincoln Sea<sup>22</sup> and Franz Victoria Strait are known to some extent, while for the region of Chukchi Plateau we have no geoacoustic data sufficiently reliable for adequate acoustic modeling. Therefore the geoacoustic characteristics of

the Lincoln Sea bottom were extended in the model to the shallow-water regions with unknown acoustic properties of the seabed.

Figure 10 demonstrates the range dependence of the amplitudes of modes 1-5 of the ACOUS signal at the central frequency along the acoustic path to the Lincoln Sea, disregarding the factor of cylindrical spreading. This pattern was calculated for a particular sound speed section that was combined from 1) the oceanographic data of a 100-km long oceanographic section across the Eurasia continental slope north of the Franz Victory Strait in 1993, 2) several temperature/salinity (T/S) profiles of the 1990s at distances from 150 to 550 km, 3) the climatology T/S profiles from 600 to 1150 km, and 4) the ICESHELF oceanographic data of 1990s in the Lincoln Sea<sup>23</sup>. The figure shows that every mode of the ACOUS signal experiences strong coupling with the other modes over the initial, shallow water section of the continental slope. The mode coupling reduces rapidly with the increase of sea depth. Relatively small variations of the temperature profiles near the edge of the continental shelf in the environmental model (such as alteration for the T/S profiles measured in 1998 for the initial 20-km section) lead to considerable changes of the modal amplitudes at the beginning of the deep-water section, which is clearly seen when comparing the modal amplitudes along the initial 100-km section shown in Fig.10 with those in Fig.11 calculated for the sound speed profiles of 1998. Note that the initial modal amplitudes (modal excitation coefficients) are not so variable under possible changes in the sound speed profile at the source location. In deeper water, at distances from 30 to 70-80 km modes 1-4 remain coupled and hence varying in amplitude due to strong horizontal gradients of the sound speed in the intermediate water layer. The coupling of modes 1-8 that contribute most to the energy of propagated signals is negligible at distances from 100 to 1000

km. Along the final section of 30-50 km long, almost every mode, except mode 1, undergoes considerable amplitude variations due to mode coupling over the Canada continental slope.

Mesoscale variations of the sound speed profile along the path, which are large enough to influence the mode coupling effects over the range-dependent sections, cause short-term variations of the modal propagation loss at the end of the path. In the presence of intense mode coupling, the amplitude variations of modes are not correlated with changes in the sound speed and have a quasi-random character. These short-term, random fluctuations may be superimposed on long-term changes in the modal propagation loss due to change in the ice statistics parameters along the path and hence the ice scattering strength. Theoretical modeling of coupled mode scattering in time varying environmental conditions is complicated, because it requires an adequate stochastic formulation of the mesoscale variations in the sound speed field for solving a complex system of stochastic differential equations for the coupled-mode propagation. For the experimental data, it may be possible to decompose the short-term variations and long-term changes by means of spectrum analysis.

As shown in Ref.20, the greater the distance from the source to the mode coupling zone, the wider the modal pulse will be on the receiving array. If the zone of intense mode coupling is far from the source and the group velocities of coupled modes are substantially different, like those of modes 1 and 2 at 20 Hz, the modal arrivals are split into multi-peak pulses. In the case of mode coupling, the pulse of a separate mode perfectly filtered on the array actually carries the energy of several modes that exchange their energy when propagating over the range-dependent sections. These modes may have different attenuation due to ice scattering over the major portion of the path. However, the resulting propagation loss of a particular mode at the receiving site will not be strictly proportional to the attenuation coefficient of this mode along the path. This makes

it more difficult to interpret the results of the propagation loss measurements for individual modes.

In the oceanographic conditions typical for the deep-water Arctic Basin, mode 1 at 20 Hz is trapped in the low-speed upper Arctic acoustic duct that is formed by the sea surface and the thermocline between the upper layer of cold Arctic water and the AIW layer. As a result, this mode propagates considerably slower and attenuates faster than the higher, mid-depth refracted modes. However, under certain environmental conditions feasible in the regions along the Eurasia continental slope north of Spitsbergen and Franz Josef Land, when the maximum AIW temperature exceeds  $2.5^{\circ}$  C, and the AIW layer expands above a 100-m depth, the upper duct cannot trap mode 1 at 20 Hz, which makes this mode propagating faster and attenuating slower than mode 2. From the modal travel times and the width of arrival pulses measured in the ACOUS signals on the Lincoln Sea array, it was concluded that such atypically warm conditions arose on the ACOUS path over a wide zone 250 - 300 km north of the source in the last quarter of 1999<sup>24</sup>. Figure 12 shows the attenuation coefficients of modes 1-5 versus frequency calculated for the typical (a) and "warm" (b) temperature and sound speed profiles observed in the Nansen Basin north of the ACOUS source (Ref. 24, Fig.6). The effective frequency band of the ACOUS signal is approximately  $20.5 \pm 1$  Hz. Hence relatively small and likely variations of the AIW characteristics lead to change of the critical frequency of modes 1 in the upper acoustic duct, which greatly affects the attenuation coefficient of this mode of the ACOUS signal. In contrast to mode 1, the attenuation of mode 2 increases in this transient frequency band. In the acoustic propagation model with the typical sound speed profiles along the path (Fig.2), such inversion in the attenuation rate of modes 1 and 2 is only seen within a short interval at the very beginning of the path (Figs 10 and 11) and does not greatly influence the total propagation loss of these

modes. However, if the warm profiles extend over 300 km, the total propagation loss of mode 1 decreases by 3-4 dB while the propagation loss of mode 2 increases by 2-3 dB.

Variations of the relative amplitudes of modes 1-5 modeled along the acoustic path to ice camp APLIS are shown in Fig.13. Mode coupling is significant for every mode along the initial section over the continental slope. The Lomonosov Ridge (at 950-1000 km) does not influence mode 1, affects slightly modes 2 and 3, and causes strong coupling of modes 4, 5 and higher. For the accepted model of bathymetry along the path, the Chukchi Rise should not influence mode 1. The other modes are subject to significant coupling over the Chukchi Rise.

#### IV. EXPERIMENTAL RESULTS

##### A. Processing of the ACOUS signals

After signal demodulation and pulse compression, the modal propagation loss can be estimated in the adiabatic approximation by<sup>25,26</sup>:

$$\begin{aligned}
 PL_m &\equiv 20 \lg \left[ \exp \left( \int_0^r \text{Im}[k_m(r', \omega_0)] dr' \right) \right] = \\
 &= 20 \lg \left( 2^{-3/2} B \sin^2 \theta A_{m0} \right) - 20 \lg (\max\{|p_m|\}) - 10 \lg(r)
 \end{aligned} \tag{2}$$

where  $p_m(t)$  is the pulse-compressed waveform of individual modes filtered on the array,  $\max\{|p_m|\}$  is the peak magnitude of the modal pulse,  $B = \sqrt{2} \exp(195/20)$  is the peak signal level of the ACOUS source,  $\theta = \pi/3$  is the phase deviation of the modulation, and

$$A_{m0} = \left( \frac{2\pi}{k_m(0, \omega)} \right)^{1/2} Z_m(0, z_0, \omega)$$

are the modal excitation coefficients that are determined from the modal eigenfunctions  $Z_m(0, z_0, \omega)$  and wavenumbers  $k_m(0, \omega)$  at the source location.

Expression (2) is exact for an ideal triangular pulse resulting after pulse compression of the phase-coded signal in an unlimited frequency band. Actually, the pulse-compressed modal arrivals filtered from the experimental signals cannot be absolutely triangular, because the frequency bandwidth of the source-to-receiver transfer functions is limited. This reduces by a considerable amount (depending on the frequency band of signal processing) the peak magnitude of the arrival pulse. Moreover, the frequency dependence of the modal wavenumbers is not absolutely linear, which may cause a widening of the modal pulse and a reduction of its maximum. The energy of the modal arrival pulse is invariant under changes in the pulse shape and hence can be used as a more accurate measure of the modal propagation loss than the maximum amplitude of the pulse. To allow for pulse distortion in equation (2), we use the effective modal amplitude  $\hat{p}_m$  instead of  $\max\{|p_m|\}$ . This effective amplitude is defined from the pulse energy

$$E_m = \int p_m(t) p_m^*(t) dt$$

as

$$\hat{p}_m = \left( \frac{3E_m}{2T} \right)^{1/2}, \quad (3)$$

where the modal pulse  $p_m$  is integrated over its whole duration and  $T$  is the length of one chip, i.e. one digit of the 255-digit M-sequence, or 10 carrier periods in our case<sup>26</sup>. Strong mode coupling also leads to a distortion of the modal pulse. In that case, the estimate of the effective modal amplitude  $\hat{p}_m$  of mode  $m$  includes the energy contribution from the other modes interacted with this mode on the propagation path.

The parameters of the Lincoln Sea array were nearly optimum for accurate spatial filtering of the 8 lower modes that contributed most to the sound field on the array. The method of mode filtering on the Lincoln Sea array is thoroughly discussed in Ref. 24, where the filtering algorithm is examined with the use of the signals numerically modeled on the hydrophones of the array. In contrast to the Lincoln Sea array, the vertical, 8-element array deployed at APLIS spanned only a relatively small section of the deep-water Arctic acoustic channel. The vertical locations of the array hydrophones were such that the matrix of modal eigenfunctions was nearly singular with respect to four of the eight eigenvalues<sup>27</sup>. Therefore the eigenvector method<sup>28</sup> was used for filtering the modes on the APLIS array. Numerical modeling showed that the results of mode filtering should be sufficiently accurate if the contribution of modes higher than 4 to the sound field is relatively small. Processing of the ACOUS signals has confirmed this assumption, which will be shown below.

#### **B. Signals on the Lincoln Sea array.**

All of the 107 ACOUS signals received on the Lincoln Sea array were processed by filtering individual modes. The modal amplitudes (energy), travel times, and phase were measured. The temporal coherence of the received signals was high so that the total gain of signal processing approached its maximum of 34 dB. The resulting signal-to-noise ratio in the post-processed signals on individual hydrophones exceeded 40 dB for almost all of the ACOUS signal recordings. The tilt of the array under variable currents was examined using the data from the pressure sensor of the micro-CTD deployed at the top of the array and a hydrodynamic model of the array mooring system. From the results of numerical modeling, it was concluded that the array tilt was negligible for mode filtering if the vertical displacement of the top sensor relative

to its uppermost position did not exceed a threshold of 0.5 m, which corresponds to horizontal displacement of approximately 20 m for the top of the Lincoln Sea array. About sixty of 107 ACOUS receptions meet this condition.

We first examined the variation of the total energy of the 8 modes filtered on the array, which is almost equivalent to the depth-integrated signal energy. All of the 107 received signals were used for this analysis, because cross-talk of the modes on the tilted array influenced the total mode energy insignificantly. Figure 14(a) demonstrates the variation in the level of the total mode energy  $\hat{p}^2 = \sum_{m=1}^8 \hat{p}_m^2$  for 14 months of observations. In the temporal variation of the modal energy one can notice long-term change in the presence of superimposed short-term fluctuations. To separate the long-term change from short-term fluctuations, we applied the wavelet de-noising procedure, decomposing the signal by the "coiflets" family wavelets. The dashed line in Fig.14(a) shows the results of such filtering. The filtered long-term change has an evident seasonal constituent with the minimum in March-April and the maximum in September-October and correlates very well with the annual cycle of changes in the mean sea ice thickness (Fig.14(b)) derived from the historical data on ice draft and the Arctic ice-ocean model<sup>11</sup>. The residual short-term variations behave as a random, delta-correlated process with a zero mean and a standard deviation of approximately 1 dB. These short-term fluctuations are relatively small, because the total mode energy is much less sensitive to changes in mode coupling due to mesoscale variations of the sound speed profiles than the energy of individual modes.

Figure 15 shows the gray-scale intensity plot of the modal arrival pulses (modes 1-3) as a function of the travel time and day of measurement. The amplitude, energy, and shape of the modal pulses underwent considerable variations during the period of observations. The short-term variations (from one transmission to the next one) were, most likely, the result of

sound speed variations at the beginning of the acoustic path over the shallow-water section of the continental slope, which influenced strongly the energy exchange of coupled modes. Mode 3 was less variable than the other modes. The amplitude of mode 1 experienced strong short-term fluctuations superimposed on noticeable long-term variations due to seasonal changes of the ice characteristics along the path. The main arrival pulse of mode 1 disappeared completely under noise in some of the ACOUS signal receptions, which happened mainly during the Arctic winter period from February to June (days 80 - 260 in Fig.15).

Figure15 also shows that the travel time of mode 1 was rapidly decreasing for the last four months of observations from 8.0 s to 6.5 s relative to the arrival of mode 3. It was concluded<sup>24</sup> that such rapid change was most likely a consequence of warmer and shallower Atlantic water masses crossing the acoustic path in the Nansen Basin within the initial 300-km section of the acoustic path north of the Eurasia continental slope, which was happening in August-December 1999. As discussed in Section III (b), the group velocity of mode 1 increases considerably under the atypically "warm" conditions, while the attenuation of this mode decreases. This is an additional factor that might have caused a 3-4-dB decrease of mode 1 attenuation over this section, and consequently a noticeable increase of the modal amplitude on the Lincoln Sea array in August-December 1999.

Variations of the effective amplitude  $\hat{p}_m$  of modes 1-3 are shown in Fig.16. Here the samplings do not include the events of excessively large tilt of the array at the time of signal reception. Since the main arrival pulse of mode 1 was greatly fluctuating, spread, and not definitely detected in some of the signal receptions, the energy of this mode was formally determined as energy of the mode-filtered signal within a time window from 5.5 s to 9 s after the arrival of mode 3. The dashed line gives the typical noise level for the filtration channel of

mode 1. The procedure of wavelet de-noising cannot be correctly applied to these data sets, because the samples are not uniformly spaced in time. Moreover, a significant number of mode 1 samples in Fig.16 do not represent the actual level of the modal energy, because they lie definitely below the noise level. Despite very large short-term fluctuations, it is evident from Fig.16 that the propagation losses of mode 1 underwent substantial seasonal variations: the pulse of mode 1 can be surely distinguished in approximately 50% of signal recordings made in October-December 1998; in February-June 1999, mode 1 almost disappeared and could be detected in very few recordings; in August 1999, the amplitude of this mode increased rapidly so that the main arrival pulse could be clearly seen in almost all of the signal recordings until the end of observations in December, which was most likely the result of superposition of the seasonal ice variations along the whole acoustic path and the rapid change in the oceanographic conditions over the initial 250-300 km section occurred in August 1999.

It is impossible to definitely observe any long-term constituent in the temporal variations of the propagation loss of modes 2 and 3, because the expected seasonal peak-to-peak variation of 2-3 dB for those modes should be hidden in the presence of the short-term fluctuations, of which the standard deviation is approximately 3 dB. The arrival pulse energy of modes 4-6 (Fig.17) also demonstrates large short-term variations. However, the seasonal cycle can be distinguished in the energy variation of these modes, especially modes 4 and 6. Note that the energy level of mode 5 is noticeably lower on average than that of mode 6, while the modal spectrum is expected to be steadily declining with the increase of the mode number for modes 4 and higher. The same peculiarity of the modal spectrum was observed in the signals that were received at ice camp Narwhal in the Lincoln Sea during the TAP experiment in 1994<sup>26</sup>. The frequency band of the ACOUS signal is close to that of the TAP signal ( $19.6 \pm 1.3$  Hz). Therefore

we assume that the minimum at mode 5 in both TAP and ACOUS signal spectra is a consequence of a specific angular dependence of the sea floor reflection coefficient at 20 Hz in the Lincoln Sea, which depends on the elastic properties of sediments and the structure of sediment layers.

Modes 2, 3, and 4 attenuate along the ACOUS path with an approximately similar rate. Therefore we calculated the total mode energy and propagation losses for the group of these modes, which allowed us to considerably reduce the short-term fluctuations due to variable effects of mode coupling. Figure 18 shows variations of the propagation loss of the group of modes 2-4 and separately mode 1 on this path during 14 months of observations. The seasonal cycle in the variation of modes 2-4 propagation losses is not prominent, but visible. In the Arctic winter period the propagation loss of this modal group was typically 3-5 dB, which is in agreement with the numerical prediction in Fig.9(a). In the summer period of 1999, the propagation loss of the modal group decreased to 1.5-2 dB on average. This number is somewhat smaller than that numerically predicted (Fig.9 (b)) for the summer ice parameters given in the caption of Fig.8. The propagation loss of mode 1 was about 19-22 dB in winter and 8-12 dB in the summer period of 1999. The propagation loss predicted numerically for summer is about 12-13 dB for the typical sound speed profiles along the path. However, if the "warm" sound speed profile extends over the initial 300-km section of the path, the predicted propagation loss of mode 1 falls to 9-10 dB.

The modal propagation loss observed in winter corresponds to the path-average attenuation coefficients of 0.015-0.018 dB/km for mode 1 and 0.003-0.004 dB/km for modes 2-4. These numbers are similar to the modal attenuation coefficients measured in the TAP experiment<sup>26</sup> on the Turpan-SIMI path, but much smaller than those measured on the Turpan-Narwhal path which

was almost coincident with the 1000-km section of the ACOUS path from the Nansen Basin to the Lincoln Sea. The integral propagation loss on the path to Narwhal was about 30 dB for mode 1 and 10-13 dB for modes 2-4. The higher signal attenuation on this path was attributed to the fact that the ice cover north of Greenland and the Canadian Archipelago was generally thicker and rougher than that in the Central Arctic Basin. The ACOUS results indicate that the winter ice cover has become considerably thinner on average in the Nansen and Fram Basins and the Lincoln Sea in 1999 relative to 1994.

It is necessary to note that the measured propagation loss of modes 2-4, which are small on this path, may have considerable relative errors due to imperfect calibration of the array hydrophones and some uncertainty in the actual level of the transmitted signal. Indeed, the calibration accuracy of the hydrophones of the Lincoln Sea array is about  $\pm 1.5$  dB. Although the amplitude of oscillations of the source membrane was automatically adjusted to the reference sound pressure with a resolution of 0.5 dB, the actual uncertainty of the absolute source level is expected to be at least  $\pm 1$  dB. Therefore the total instrumental error of the absolute propagation loss measurements may amount to 2-5 dB, especially as some of the instrumental errors contain regular components.

### **C. Signals on the APLIS array**

The arrival patterns of modes 1-4 of the ACOUS signal filtered on the vertical array at ice camp APLIS on 9 and 13 April 1999 are shown in Figs. 19 (a) and (b) respectively. The amplitude of mode 1 shown in this figure is multiplied by a factor of 2. Mode 2 is the dominant mode in the ACOUS signals received at APLIS. The arrival pulse of this mode in the first signal is split, which testifies to strong mode coupling. As follows from the width of the split pulse and the

results of numerical modeling, strong coupling of mode 2 with the higher modes occurred along the final section of the propagation path over the Chukchi Plateau. In contrast to the numerical prediction shown in Fig.19(c), the arrival pulse of mode 3 in these signals was very weak and deformed due to bottom interaction and mode coupling over the Chukchi Plateau. The arrival pulse of mode 1 is weak, but distinguishable in both signals. Mode 4 is practically vanishing in these signals.

The propagation loss of mode 1 measured on the APLIS array is 41 dB for the first signal and 45 dB for the second signal, which corresponds to the path-average attenuation coefficients of 0.015 dB/km and 0.0165 dB/km respectively. These numbers are similar to the propagation loss and attenuation coefficients of mode 1 measured on the Turpan-SIMI path in the TAP experiment ( $43.5 \pm 2.5$  dB and  $0.0165 \pm 0.001$  dB/km respectively). Moreover, the path-average attenuation coefficients of mode 1 measured in April 1999 on both ACOUS paths are approximately the same. In contrast to mode 1, the propagation losses of mode 2 in the two ACOUS signals received at APLIS are much larger than that measured in the TAP experiment on the Turpan-SIMI path. For the first, adiabatic arrival pulse of mode 2, the propagation loss was approximately 21 dB and 24 dB in these two ACOUS signals, versus  $13 \pm 1.5$  dB measured in the TAP experiment. The path-average attenuation coefficient of this mode estimated on the path to APLIS is 0.008-0.009 dB/km, which is approximately two times higher than that measured on the ACOUS path to the Lincoln Sea. The excessive attenuation of mode 2 on this path was, most likely, the result of strong interaction of this mode with the sea floor in the region of the Chukchi Plateau. The evidence of strong mode coupling for mode 2 and lack of mode 3 in the ACOUS signals received at APLIS support this assumption. An obvious discrepancy between the experimental and modeled arrival patterns of modes on the APLIS array is probably a result of

incorrect modeling of the bathymetry and elastic properties of the sea floor along the section of the acoustic path over the Chukchi Plateau.

### **Conclusions**

The ACOUS experiment has proven the capability of low-frequency cross-Arctic acoustic transmissions to observe long-term basin-scale changes in the Arctic ice cover. The seasonal cycle in the variations of the total energy losses of the transmitted signal and the propagation losses of individual modes was observed. According to the theory of ice scattering, coherent losses of the low frequency signals propagated under ice in the Arctic Ocean depend primarily on the height and correlation length of the ice roughness. As proven by numerous upward-looking sonar observations of Arctic ice draft, the height of ice roughness closely mirrors the change in the mean ice thickness through a nearly linear relationship. For ice draft in excess of 1 m, the standard deviation of the bottom ice boundary is about 0.5-0.6 of the mean ice thickness. Seasonal melting and growing of sea ice result basically in variations of the mean ice thickness and standard deviation of ice roughness, which influences considerably the acoustic propagation losses and hence can be observed by means of long-range acoustic transmissions, as was done in the ACOUS experiment.

The results of propagation loss modeling along the ACOUS path to the Lincoln Sea, using the most recent ice draft data and the model of seasonal change of ice thickness, are basically in agreement with the results of experimental observations on this path. This allows us to derive the correlation between the modal propagation loss and ice thickness and hence gives a way to build an acoustic inversion method for remote observations of ice thickness. However, the accuracy of such acoustic monitoring of Arctic sea ice needs to be examined in the future experiments by

means of ice draft profiling conducted along the acoustic path at the time of acoustic observations.

Numerical modeling has shown that the sound speed profile influences considerably the attenuation of individual modes due to ice scattering. Recent oceanographic observations and the ACOUS results give evidence of large-scale spatial and temporal variations of the sound speed profile in the Arctic Ocean. Therefore modelers and experimental researchers should take into account the dependence of acoustic transmission losses on the sound speed profile when developing acoustic propagation models and planning acoustic experiments in the Arctic.

Attenuation of mode 1 at 20 Hz is much more sensitive to changes of the ice cover than the higher modes. Remote observations of Arctic sea ice by means of low frequency cross-Arctic acoustic transmissions would be much more accurate, if mode 1 is not subject to significant interaction with the sea floor and strong coupling with the higher modes due to variable bathymetry and horizontal changes in the sound speed profile. Such propagation conditions for mode 1 can be achieved through choosing either better locations of the source and the receiving array or a more suitable frequency band of the signal. For example, at 23 Hz mode 1 would experience somewhat weaker interaction with the sea floor along the initial section of the ACOUS path and much less significant coupling with the higher modes over the frontal zone in the Nansen Basin than that observed at 20.5 Hz in the ACOUS experiment.

### **Acknowledgements**

This work was supported by the Office of Naval Research and the Civilian Research and Development Foundation (award #RG2-2407). The authors would like to express their deep appreciation to John M. Lents of SAIC who managed field operations in the ACOUS

experiment. The author also thanks Vladimir Kudryashov for valuable suggestions and comments in relation to the algorithm for numerical modeling of the coherent acoustic reflection from Arctic sea ice.

## References

- <sup>1</sup> B.M. Buck and C.R. Green, "Arctic deep-water propagation measurements", *J. Acoust. Soc. Am.*, **36**, pp.1526-1533 (1964);
- <sup>2</sup> F. DiNapoli and R. Mellen, "Low frequency attenuation in the Arctic Ocean", in *Ocean Seismo-Acoustics*, edited by T. Akal and J.M. Berkson (Plenum NY, 1986), pp. 387-395;
- <sup>3</sup> E. Livingston and O. Diachok, "Estimation of average under-ice reflection amplitudes and phases using matched-field processing", *J. Acoust. Soc. Am.*, **86**(5), pp.1909-1919 (1989);
- <sup>4</sup> P.N. Mikhalevsky, A.B. Baggeroer, A.N. Gavrilov, and M.M. Slavinsky, "Experiment Tests Use of Acoustics to Monitor Temperature and Ice in the Arctic Ocean", *EOS*, **76**, No.27, pp. 265-269 (1995);
- <sup>5</sup> R. Pawlowicz, D. Farmer, B. Sotirin, and S. Ozard, "Shallow-water receptions from the transarctic acoustic propagation experiment", *J. Acoust. Soc. Am.*, **100**, pp.1482-1492 (1996);
- <sup>6</sup> G. Duckworth, K. LePage, and T. Farrel, "Low-frequency long-range propagation and reverberation in the Central Arctic: Analysis of experimental results", *J. Acoust. Soc. Am.*, **110**(2), pp.747-760 (2001);
- <sup>7</sup> B. Rudels, E.P. Jones, L.G. Anderson, and G. Kattner, "On the intermediate depth waters of the Arctic Ocean", in *The Polar Oceans and their Role in Shaping the Global Environment* edited by Johannessen *et al.* (American Geophysical Union, Washington D.C., 1994), pp. 33-46;
- <sup>8</sup> K. Aagaard, "A synthesis of the Arctic Ocean circulation", *Rapports et Proces-Verbaux des Reunions du Conseil International pour l'Exploration de la Mer*, **188**, pp. 11-22 (1989);
- <sup>9</sup> Environmental Working Group (EWG): Joint U.S. Russian Atlas of the Arctic Ocean (CD-ROM), National Snow and Ice Data Center, Boulder, CO (1998);

- <sup>10</sup> D. Cavalieri, P. Gloerson, and J. Zwally: 1990 - March 2000 DMSP SSM/I daily polar gridded sea ice concentrations; edited by J. Maslanik and J. Stroeve, Boulder, CO: National Snow and Ice Data Center. Digital media: <http://nsidc.org/data/nsidc-0002.html>;
- <sup>11</sup> D.A. Rothrock, Y.Yu and G.A. Maykut, "Thinning of the Arctic sea-ice cover", *Geo. Res. Let.*, **26**(23), pp. 3469-3472 (1999);
- <sup>12</sup> National Snow and Ice Data Center: Submarine upward looking sonar ice draft profile data and statistics. Digital data from: [nsidc@kryos.colorado.edu](mailto:nsidc@kryos.colorado.edu). NSIDC, University of Colorado at Boulder;
- <sup>13</sup> R.H. Bourke and A.S. McLaren, "Contour mapping of Arctic Basin ice draft and roughness parameters", *J. Geophys. Res.*, **97**(C11), pp.17715-17728 (1992);
- <sup>14</sup> V.M. Kudryashov, "Sound reflection from ice cover", *Phys. Acoustics*, **42**(2), pp. 247-253 (1996);
- <sup>15</sup> A.N. Gavrilov, "Study of acoustic propagation loss in the Arctic Ocean using the data of the ACOUS experiment", Tech. Rep., Western Services Corp. for ONR, Moscow, 2002;
- <sup>16</sup> K. LePage and H. Schmidt, "Modeling of low-frequency transmission loss in the central Arctic", *J. Acous. Soc. Am.*, **96**(3), pp.1783-1795 (1994);
- <sup>17</sup> J. Goff and T. Jordan, "Stochastic modeling of seafloor morphology: version of Sea Beam data for second order statistics", *J. Geophys. Res.*, **93**, pp. 13589-13608 (1988);
- <sup>18</sup> W.A. Kuperman and H. Schmidt, "Self-consistent perturbation approach to rough surface scattering in stratified elastic media", *J. Acous. Soc. Am.*, **86**(4), pp.1511-1522 (1989);
- <sup>19</sup> M.B. Porter, "The KRAKEN normal mode program", Tech. Rep., SACLANT Undersea Research Center Mem. (SM-245)/ NRL Mem. Rep. 6920 (1991);

- <sup>20</sup> A.N. Gavrilov and P. N. Mikhalevsky, "Mode-coupling effects in acoustic thermometry of the Arctic Ocean", in *Inverse Problems in Underwater Acoustics*, edited by M. Taroudakis and G. Makrakis (Springer-Verlag NY, 2001), pp.105-125;
- <sup>21</sup> International Bathymetric Chart of the Arctic Ocean: <http://www.ngdc.noaa.gov/mgg/bathymetry/arctic/arctic.html> (2001);
- <sup>22</sup> W.H. Geddes, "Geoacoustic model of the Lincoln Sea", GGAI Tech. Rep. 3-90 (1990);
- <sup>23</sup> J.L. Newton and B.J. Sotirin, "Boundary undercurrent and water mass changes in the Lincoln Sea", *J. Geo. Res.*, **102**(C2), pp. 3393-3403 (1997);
- <sup>24</sup> A.N. Gavrilov and P.N. Mikhalevsky, "Recent results of the ACOUS (Arctic Climate Observations using Underwater Sound) Program ", *Acta Acustica united with Acustica*, **88**,(5), pp.783-791 (2002);
- <sup>25</sup> A.N. Gavrilov and P.N. Mikhalevsky, "Phase acoustic tomography with broadband signals in the Arctic", *Proc. of 3-th ECUA Conf.*, Heraklion, Crete, 1996, pp.851-856;
- <sup>26</sup> P.N. Mikhalevsky, A.N. Gavrilov, and A.B. Baggeroer, "The Transarctic Acoustic Propagation Experiment and climate monitoring in the Arctic", *IEEE J. Oceanic Eng.*, **24**(2), pp. 182-202 (1999);
- <sup>27</sup> P.N. Mikhalevsky and A.N. Gavrilov, "Acoustic thermometry in the Arctic Ocean", *Proc. 5-th European Conf. on Underwater Acoustic*, Lyon, France, 2000, v.2, pp.1291-1296;
- <sup>28</sup> T.C. Yang, "A method of range and depth estimation by modal decomposition", *J. Acous. Soc. Am.*, **82**(5), pp.1736-1745 (1987);

### Figure captions

**Fig. 1.** ACOUS experiment paths in the Arctic Ocean. The salmon-colored lines and arrows show the recently proposed scheme of Atlantic water circulation<sup>7</sup>. The blue-colored lines and arrows show the same but for the Pacific water circulation.

**Fig. 2.** Bathymetry and the typical sound speed profile along the acoustic path to the Lincoln Sea.

**Fig. 3.** Bathymetry and the sound speed profile along the acoustic path to APLIS.

**Fig. 4.** Histograms of the fall-off rate of the ice roughness power spectra calculated for the ice draft profiles that were observed in the spring of 1991 (a, total length of profiles 3500 km) and the autumn of 1996 (b, total length of profiles 5350 km). The ice roughness spectrum was calculated for every profile section. The length of sections varied from several km to 50 km.

**Fig. 5.** One of the ice roughness power spectra measured in 1991 (dashed line and dots) and its approximation by a model Goff-Jordan spectrum with a 2-D fractal dimension of 2.5 (solid line).

**Fig. 6.** Histograms of the ice roughness correlation length calculated for the ice draft profiles that were observed in the spring of 1991 (a) and the autumn of 1996 (b).

**Fig. 7.** Same as Fig.6, but for the ratio of roughness standard deviation and mean ice thickness.

**Fig. 8.** Coherent reflection coefficient versus grazing angle at frequencies 16, 20, 24, 28, 32, and 36 Hz for Arctic sea ice with the typical winter parameters (a: mean thickness = 3.0 m; standard deviation of bottom ice boundary = 1.8 m; standard deviation of top ice boundary = 0.45 m; correlation length = 40 m) and the typical summer parameters (b: mean thickness = 2.0 m;

standard deviation of bottom ice boundary – 1.2 m; standard deviation of top ice boundary – 0.3 m; correlation length – 40 m). The following acoustic properties of ice were used in the model: compressional wave velocity – 3000 m/s; shear wave velocity – 1800 m/s; compressional wave attenuation – 0.45 dB/λ; shear wave attenuation – 0.9 dB/λ; relative density – 0.91.

**Fig. 9.** Attenuation coefficients of modes 1-5 at 20.5 Hz along the ACOUS path and the resulting propagation loss (PL) modeled for the winter (a) and summer (b) ice conditions corresponding to the ice reflection coefficient shown in Figs.8 (a) and (b) respectively. This model prediction was obtained using the sound speed profiles along the ACOUS path typical in 1990s.

**Fig. 10.** Modeled variations of the amplitudes of modes 1-5 at the central frequency of the ACOUS signal along the path to the Lincoln Sea, disregarding cylindrical spreading (section from 100 to 1000 km is not shown). The sound speed vertical section along the path was combined from 1) the oceanographic data of a 100-km long oceanographic section across the Eurasia continental slope north of the Franz Victory Strait in 1993, 2) several temperature/salinity (T/S) profiles of the 1990s at distances from 150 to 550 km, 3) the climatology T/S profiles from 600 to 1150 km, and 4) the ICESHELF oceanographic data of 1990s in the Lincoln Sea.

**Fig. 11.** Variations of the amplitudes of modes 1-5 at the central frequency along the initial 100-km section of the ACOUS path modeled for the sound speed profiles observed in 1998 at distances up to 20 km north of the acoustic source and the sound speed profiles measured in 1993 in the deep-water part of this section.

**Fig. 12.** Attenuation coefficients of modes 1-5 versus frequency for the ice reflection coefficient shown in Fig.8(b) and the typical (a) and “warm” (b) sound speed profiles shown in Ref. 25, Fig.6.

**Fig. 13.** Modeled variations of the amplitudes of modes 1-5 at the central frequency of the ACOUS signal along the path to APLIS, disregarding cylindrical spreading. The sound speed vertical section along the path was combined from 1) the historical oceanographic data of 1990s for the initial 350-km section of the path and 2) the SCICEX-1999 T/S profiles observed along the major section from 350 km to 2720 km.

**Fig. 14.** (a) - Variations of the total energy of modes 1-8 filtered on the Lincoln Sea array. The dashed line shows the result of wavelet filtering of the long-term component of variations. (b) - Modeled seasonal cycle of ice draft (dashed) and thickness (solid) <sup>11</sup>.

**Fig. 15.** Gray-scale intensity plot of the modal arrival pulses (modes 1-3) as a function of the travel time and the day of measurements. The signals are synchronized with the arrival time of mode 3 shown by a dashed line.

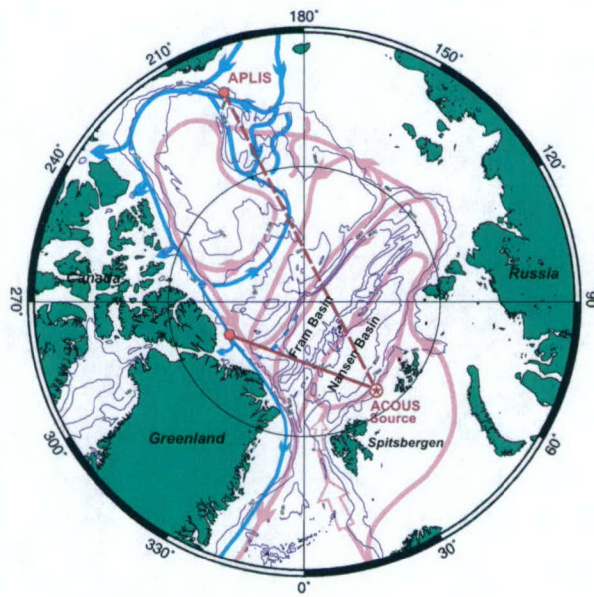
**Fig. 16.** Variations of the energy of modes 1 (blue), 2 (green), and 3 (red) filtered on the Lincoln Sea array during the ACOUS experiment. The dashed line shows the typical noise level in mode 1 filtered channel.

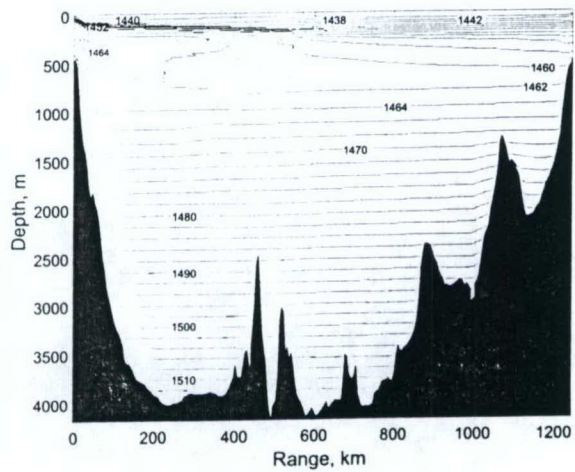
**Fig. 17.** Same as Fig.16, but for modes 4 (blue), 5 (green), and 6 (red).

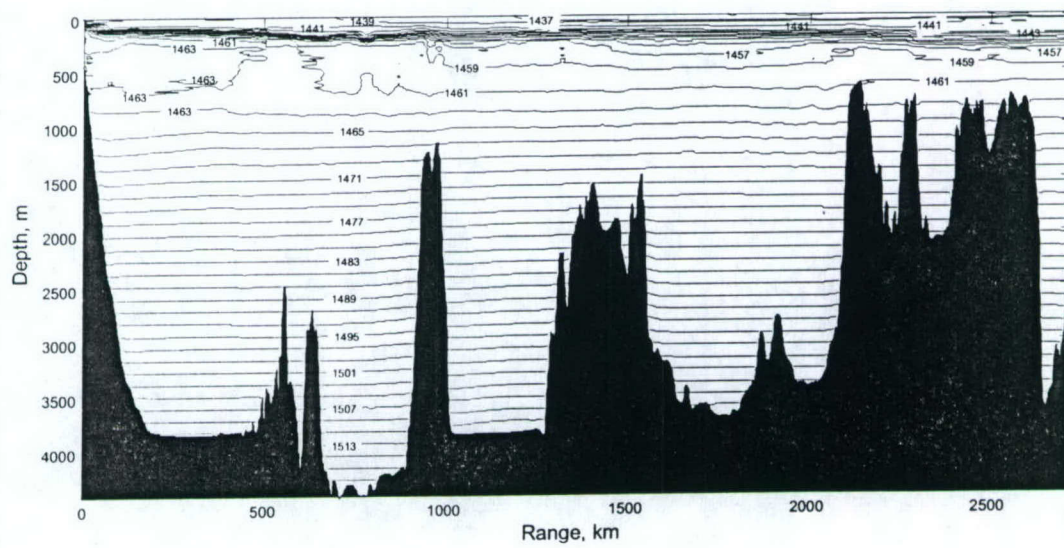
**Fig. 18.** Propagation loss of mode 1 (blue) and the group of modes 2-4 (red) received on the Lincoln Sea array during the ACOUS experiment. The estimates of mode 1 propagation loss

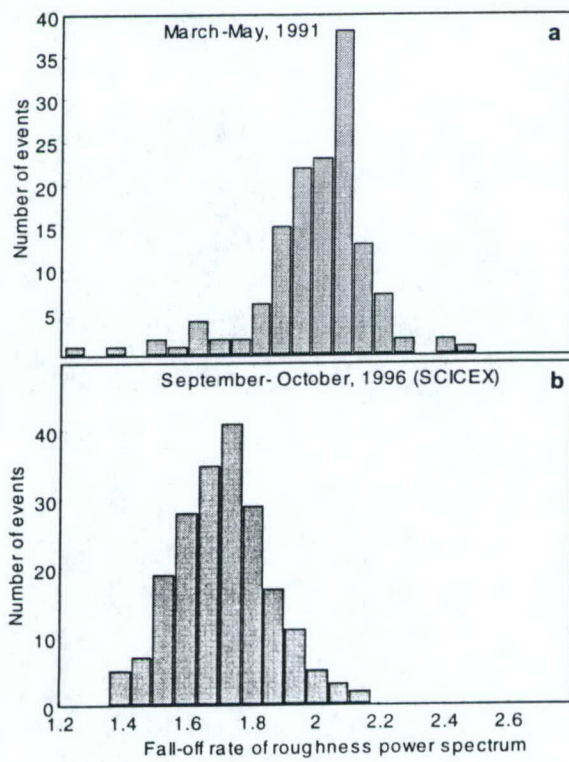
above the dashed line are erroneous and hence are not shown, because they were obtained at too low signal-to-noise ratio.

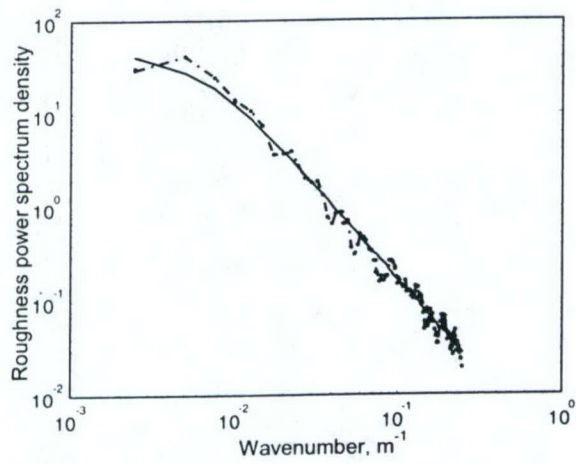
**Fig. 19.** The arrival patterns of modes 1-4 of the ACOUS signal filtered on the vertical array at ice camp APLIS on 9 April at range  $R = 2714.84$  km from the source (a) and 13 April at range  $R = 2722.44$  km (b). The bottom panel (c) shows the modeled arrival patterns of modes 1-6 of the ACOUS signal on the APLIS array at  $R = 2722.44$  km. The amplitude of mode 1 is shown doubled in all three plots.

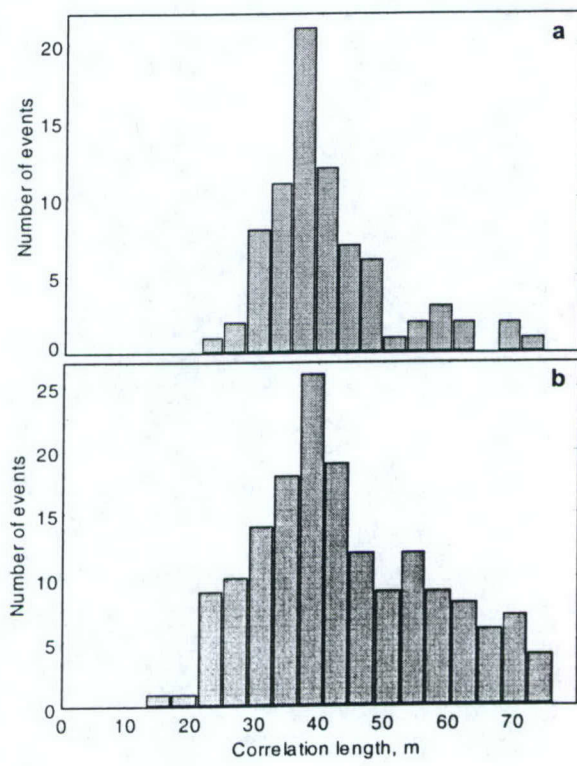


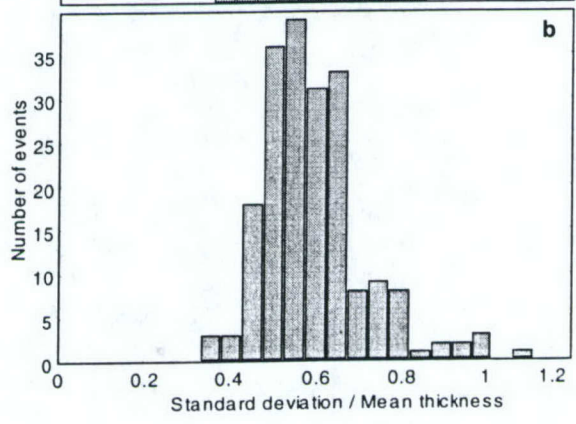
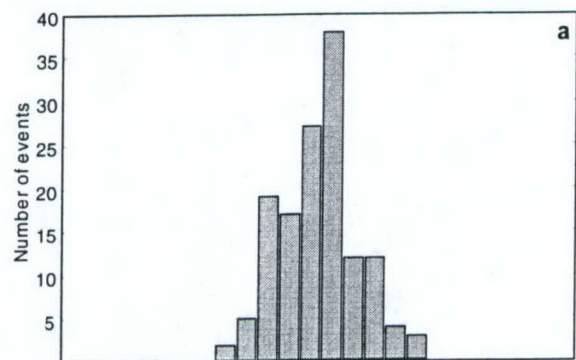


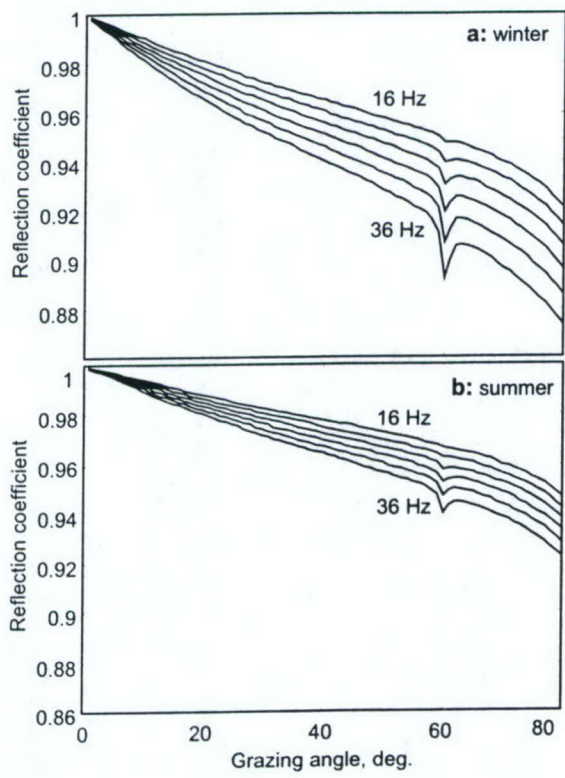


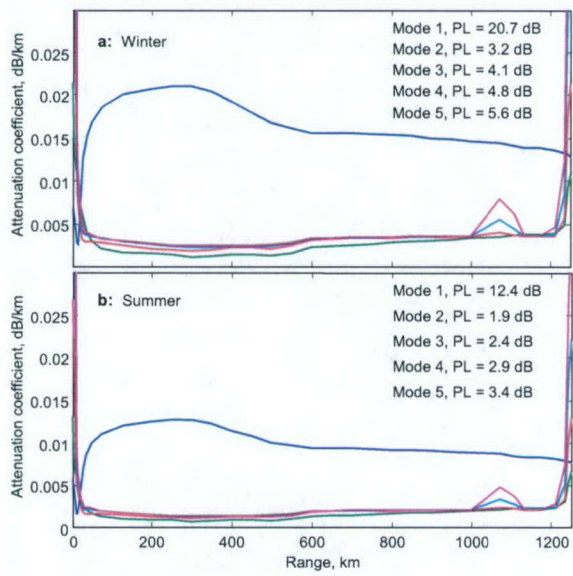


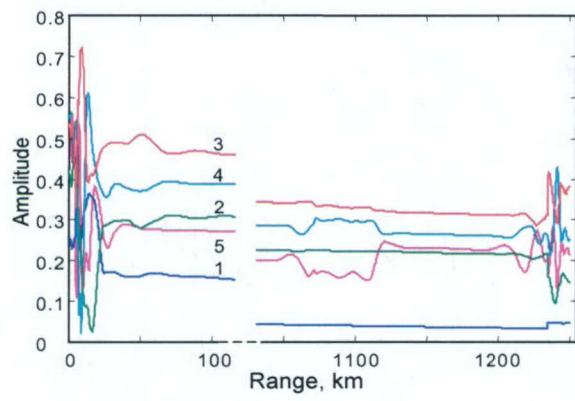


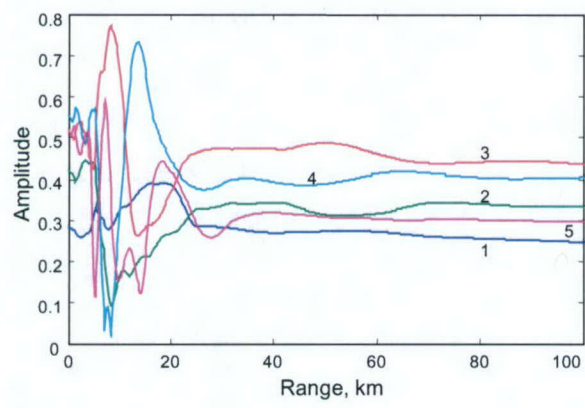


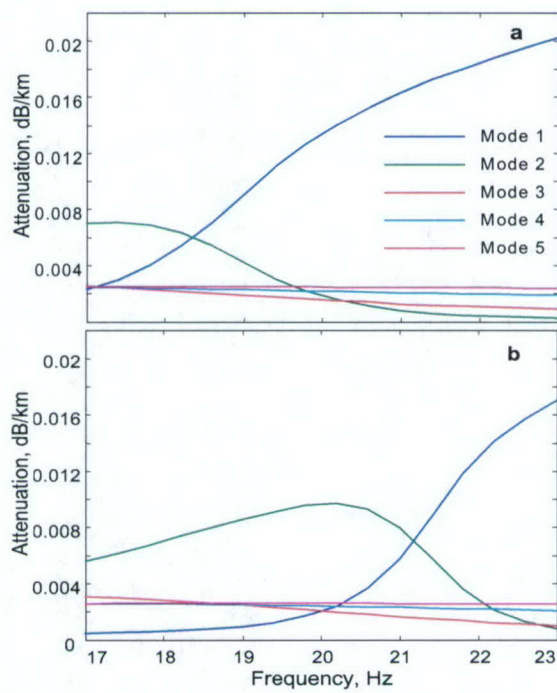


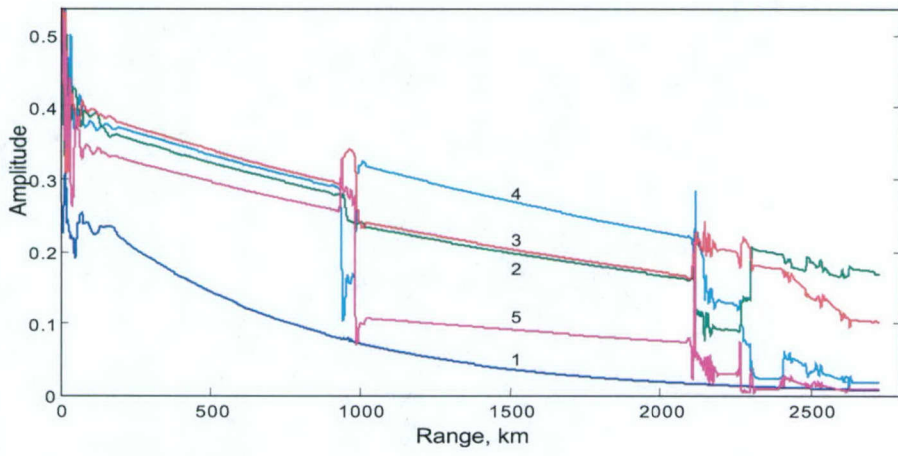


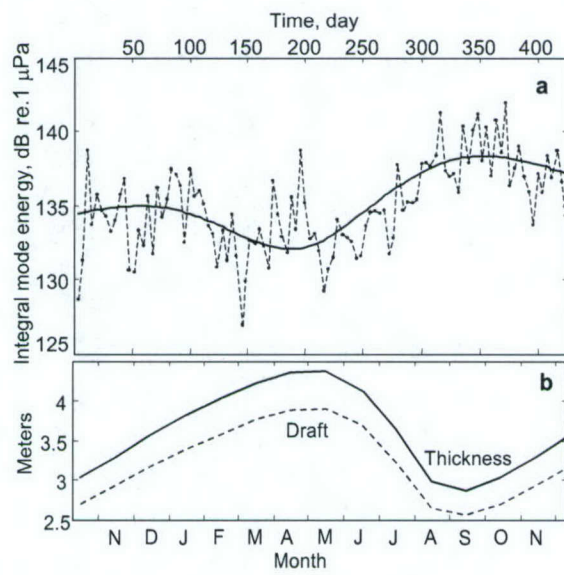


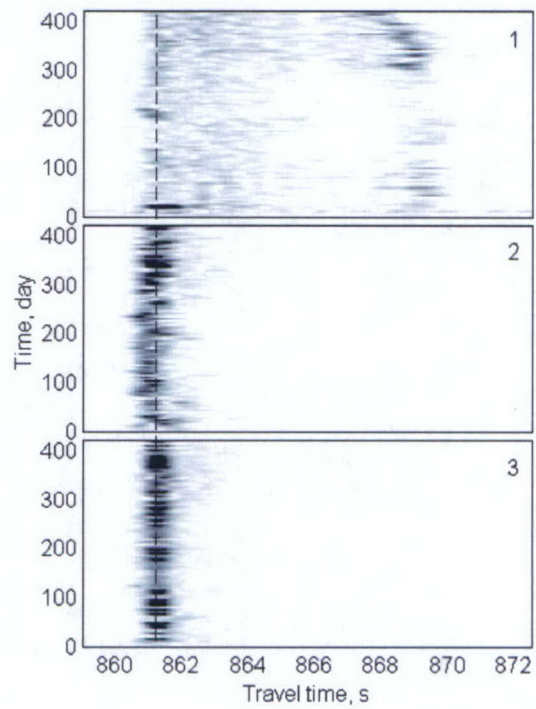


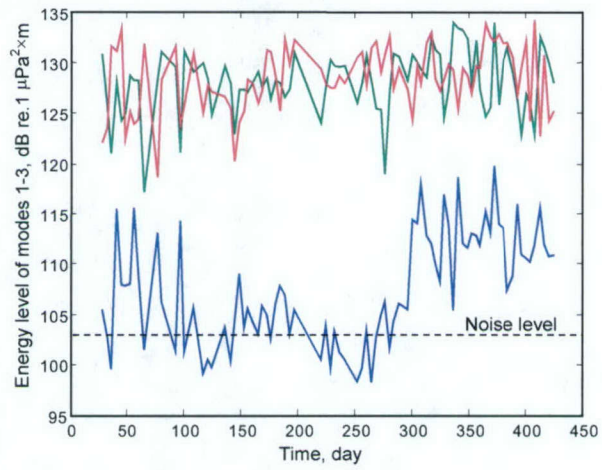


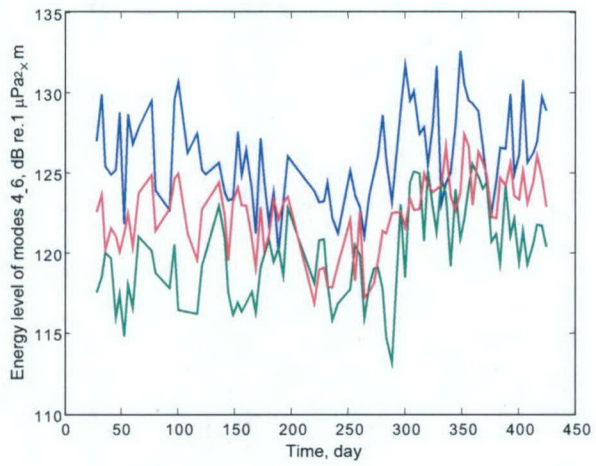


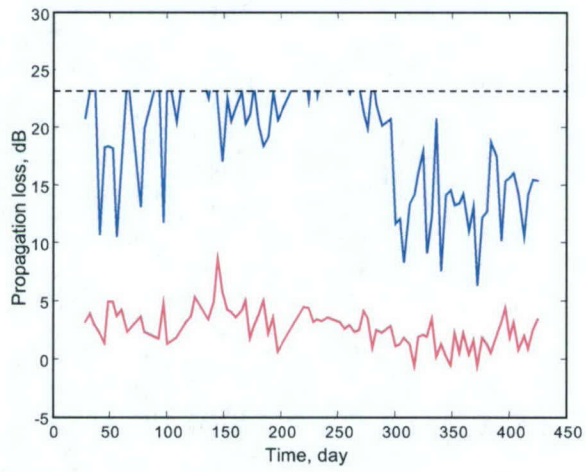


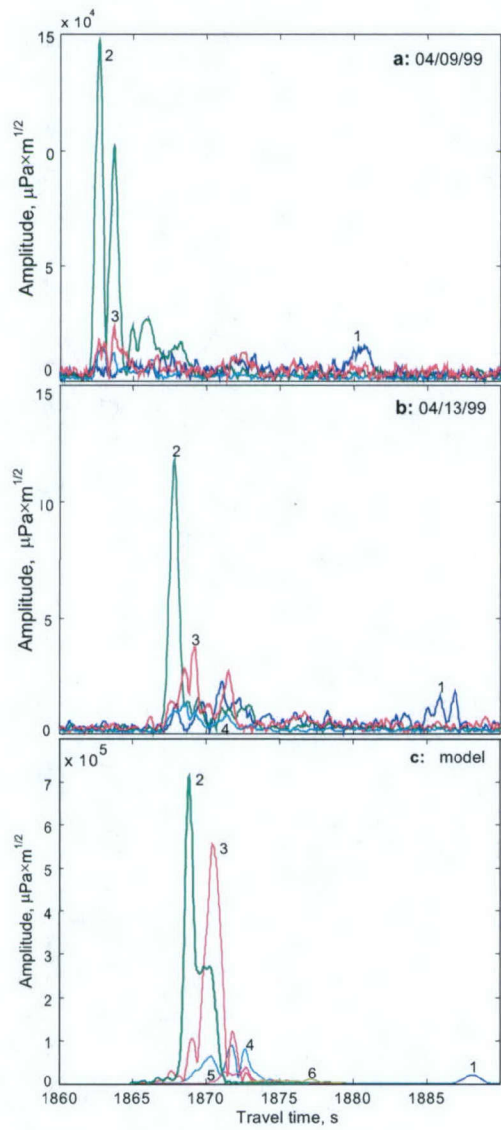












# Achievements and a Potential Role of Underwater Acoustics in Studying Large-Scale Changes in the Arctic Ocean

A.N. Gavrilov, Curtin University of Technology, Australia

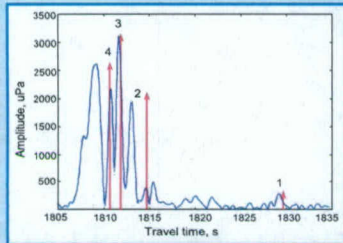
P.N. Mikhalevsky, Science Applications International Corporation, USA

V.V. Goncharov and Yu.A. Chepurin, Shirshov Institute of Oceanology, Russia

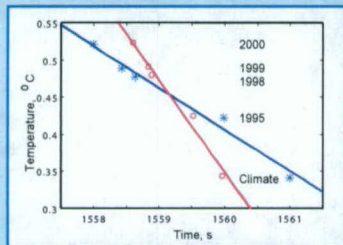
K.D. Sabinin, Andreyev Acoustics Institute, Russia

## ABSTRACT

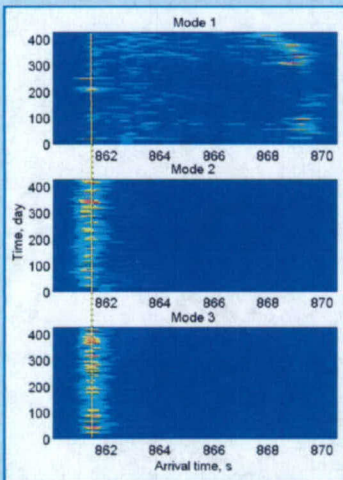
The Transarctic Acoustic Propagation experiment in 1994 revealed integral, basin-scale warming of the Atlantic intermediate water layer relative to climatology, which supported the earlier observations of warming in this layer in certain regions of the Arctic Ocean. Both experimental and modeling results have shown that the travel time of individual modes of a low-frequency acoustic signal is a precise indicator of changes in the integral Atlantic water temperature along cross-Arctic sections. The first long-term stationary system of Arctic acoustic thermometry was experimentally tested for 14 months in 1998-1999 in the framework of the Arctic Climate Observations using Underwater Sound (ACOUS) program. Remote acoustic observations on the cross-Arctic path from Franz Josef Land to the Lincoln Sea detected substantial warming of Atlantic waters and a shoaling of the thermocline that occurred rapidly in the central Nansen Basin (83-840 N, 20-300 E) in the last quarter of 1999. The long-term acoustic transmissions in 1998-1999 were also capable of detecting seasonal variations of the mean thickness of sea ice along the cross-Arctic path. At present, an extensive network of acoustic thermometry paths for multiyear observations in the Arctic Ocean is projected. The feasibility of acoustic halinometry, i.e. remote observations of salinity change in the upper layer, is also examined by numerical modeling.



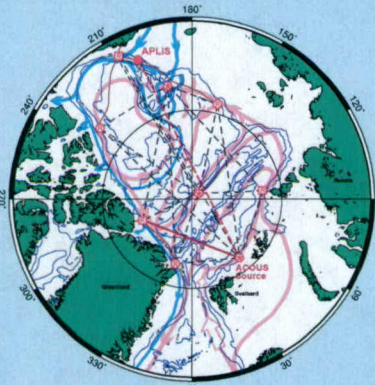
The arrival pattern of the signal received at ice camp SIMI in the Transarctic Acoustic Propagation experiments in April 1994 (blue), and the arrival times and amplitudes of modes 1-4 (red arrows) numerically modeled with the use of climatology oceanographic data for 1970s. Difference in the experimental and modeled travel times of mode 2 of approximately 2 s indicates warming of almost 2 °C in the section-average temperature of the Atlantic water layer along the acoustic path.



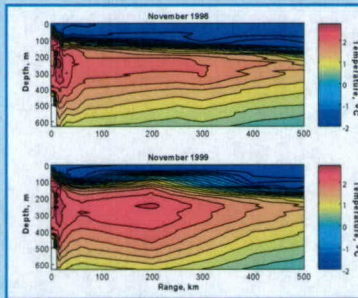
The section-average temperature of the AW layer derived from the SCICEX transect of different years and the climatology data versus the travel time of modes 2 (stars) and 3 (circles) of an acoustic signal at 20.5 Hz propagated over the SCICEX section, and the best linear fit for the relationship between these characteristics.



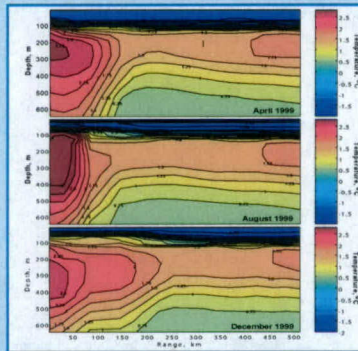
The amplitude of modes 1-3 arrival pulses as a function of the travel time and the day of measurements. Considerable long-term variations of the travel time, amplitude, and pulse width of mode 1 indicated large-scale changes in the Atlantic water temperature and the thermocline depth over the initial 300-km section of the acoustic path. The variations of mode 2 travel time due to those changes are also noticeable, but not so large.



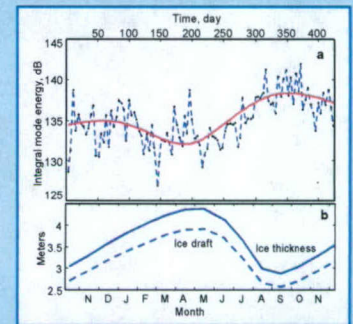
Acoustic observations on the ACOUS acoustic path to the Lincoln Sea (solid red line) were conducted for 14 months in 1998-1999. Two of the 107 ACOUS signals were received at ice camp APLIS. The acoustic path to APLIS (dashed red line) was close to the SCICEX transects conducted in 1995, 1998, 1999, and 2000. A notional monitoring grid for the Arctic Ocean is shown by black dashed lines. This network is called ATAM, which stands for Acoustic Thermometry and Autonomous Monitoring. In addition to acoustic receive arrays, the ATAM moorings are planned to equip with oceanographic, biological, chemical, sea ice, and seismic sensors. The sea-shore interface in the Lincoln Sea already exists. Such an interface in the Beaufort Sea does not yet exist.



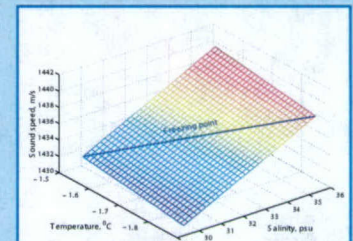
The temperature section shown in the upper panel was modeled using the oceanographic data collected along the initial 500-km section of the ACOUS path in the 1990s. The ACOUS signal parameters observed in the beginning of the experiment are in agreement with this profile. The bottom panel demonstrates the temperature section that was obtained by inversion of the modal characteristics of the ACOUS signals received in late November - December 1999.



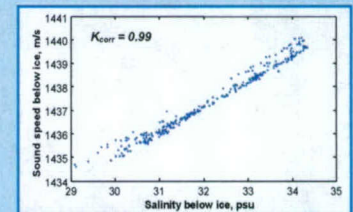
The temperature sections along the initial 500-km section of the ACOUS path in April, August, and December of 1999 derived from the results of numerical simulation using the MOM-2 ocean model by the Geophysical Fluid Dynamics Laboratory [Karcher et al., JGR, v.108, C2]. Note that the model also shows substantial shoaling of the thermocline at the end of 1999.



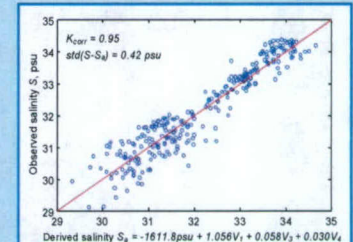
a: Variations of the total energy of modes 1-8 filtered on the Lincoln Sea array. The red line shows the result of wavelet filtration of the long-term component of variations; b: modeled seasonal cycle of ice draft (dashed) and thickness (solid) [D.A. Rothrock et al., GRL, v.28(23), pp. 3469-3472]. A seasonal component can be clearly seen in the acoustic data. The numerically modeled change of the modal propagation loss due to seasonal variations of the ice thickness corresponds to the observed data.



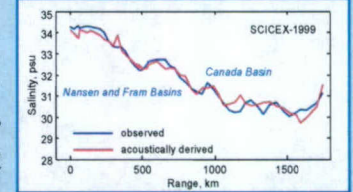
Sound speed in sea water at low temperatures. At freezing point, the sound speed varies mainly with the water salinity.



Correlation between the mean salinity and sound speed in the upper 30-m water layer below ice in the Arctic Ocean.



Correlation between the observed salinity of the upper layer and the results of acoustic inversion using the propagation speed V of modes 1, 3, and 4 at 90 Hz.



The mean salinity of the upper 30-m water layer obtained from the SCICEX-1999 oceanographic transect (blue), and the results of acoustic inversion for salinity using the travel times of modes 1, 3, and 4 at 90 Hz over short sections along the transect.

## CONCLUSIONS

1. The first detection of current warming of Atlantic waters on a basin scale in the Arctic Ocean was made by means of acoustic thermometry in the TAP experiment in 1994.
  2. Long-term acoustic observations conducted in the ACOUS experiment in 1998-1999 revealed dramatic change that occurred in the water masses in the Nansen Basin north of the Franz Victory Strait in August-December of 1999. According to the ACOUS results, the Atlantic layer become considerably thicker and warmer and the thermocline rose above a 100-m depth in the Nansen Basin 150-300-km north of the Eurasia continental slope.
  3. The ACOUS experiment has proven the capability of low-frequency cross-Arctic acoustic transmissions to observe long-term basin-scale changes in the Arctic ice cover. The seasonal cycle in the variations of the total energy losses of the transmitted signal and the propagation losses of individual modes was observed.
  4. The results of numerical modeling show that change in the integral salinity of the upper under-ice layer can be remotely observed by means of acoustic transmissions at frequencies of 80-100 Hz. The accuracy of such measurements is a subject of further studies.
- The work was funded by the National Science Foundation (Office of Polar Programs), the Office of Naval Research (High Latitude Programs), the U.S. Civilian Research and Development Foundation (Award No. RG2-2407), RFBR Grant 02-05-64339, and the Ministry of Industry, Science, and Technology of the Russian Federation H11-1277.2003.5.